ChemComm

COMMUNICATION

View Article Online
View Journal | View Issue

Cite this: *Chem. Commun.*, 2017, **53**, 740

Received 25th October 2016,
Accepted 14th December 2016

DOI: 10.1039/c6cc08598a

www.rsc.org/chemcomm

Porous nanopeapod Pd catalyst with excellent stability and efficiency†

Xuecheng Chen,*[ab] Chao Zhang,[a] Ryszard J. Kalenczuk,[b] Paul K. Chu,[c] Dengsong Zhang,*[d] Tao Tang*[a] and Ewa Mijowska[b]

Porous Pd@m-C/SiO_2 nanopeapods are prepared by a nanoconfinement method. The Pd nanoparticles show high efficiency and stability in chemical reactions such as reduction of nitrobenzene by H_2 and reduction of NO by NH_3. The high catalytic activity is attributed to the unique peapod structure, mesoporous wall, and large specific surface area on Pd@m-C/SiO_2 rendering the Pd nanoparticles highly active in chemical reactions.

Design of new-generation catalysts with high activity, selectivity, and resistance to deactivation is an important objective of scientific research and applications.[1–4] In recent years, nanotechnology has played essential roles in many scientific fields. For instance, nanoparticles made of platinum-group metals have been studied as primary catalysts in low-temperature reduction of automobile pollutants, olefin hydrogenation, dehydrogenation reaction, and Suzuki coupling reaction.[5–10] The thermal and chemical stability of nanoparticulate catalysts is crucial to the catalytic performance. However, metal nanoparticles can easily deform and aggregate because of the high surface energy and the catalytic efficacy of metal nanoparticles deteriorates during chemical reactions.[11] Unfortunately, many industrial catalytic processes are carried out at high temperature and consequently, nanoparticle catalysts with long-term stability at high temperature are highly needed.[12–19] The main reasons for deactivation is that organic species cover the catalyst surface leading to loss of precious metals and growth of metal particles[20] and it is challenging to design catalysts with long-term stability, efficiency, and selectivity.

In this work, peapod Pd@m-C/SiO_2 is embedded with Pd nanoparticles to improve the thermal stability. The outer mesoporous C/SiO_2 layer prevents Pd nanoparticles from sintering and protects the Pd nanoparticles during catalytic reactions at high temperature. The mesoporous C/SiO_2 wall has a large specific surface area allowing more reactants to access the Pd nanoparticles and high catalytic activity. Preparation of the catalyst is relatively easy compared to commercial Pd/AC catalysts. To demonstrate the catalytic activity of the materials, two chemical reactions are conducted and the catalyst shows excellent long-term stability and high activity during the reactions.

The peapod Pd@m-C/SiO_2 nanotubes are prepared in three steps as illustrated in Fig. 1: (1) deposition of Pd nanoparticles on carbon nanotubes (CNT/Pd), (2) deposition of a mesoporous silica layer on CNT/Pd to produce the CNT/Pd@m-SiO_2 mesostructure, and (3) annealing at a high temperature under Ar to produce the peapod Pd@m-C/SiO_2. The peapod Pd@m-C/SiO_2 consists of Pd nanoparticles and a mesoporous C/SiO_2 layer.

The Pd nanoparticles are characterized by TEM. The Pd nanoparticles have a mean diameter of 2.5 nm and are densely and mono-dispersed on the CNTs (Fig. 2a). After the sol–gel process, a mesoporous silica layer is formed on the CNT/Pd structure as shown in Fig. 2b. The small black dots are Pd nanoparticles and the thickness of the mesoporous layer is about 20 nm. After annealing in Ar, the Pd@m-C/SiO_2 structure is formed as shown in Fig. 2c, d and Fig. S1 (ESI†). In the

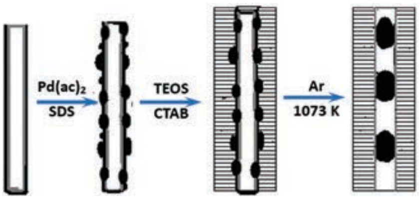

Fig. 1 Schematic showing the preparation of the peapod Pd@m-C/SiO_2.

---

[a] *State Key Laboratory of Polymer Physics and Chemistry, Changchun Institute of Applied Chemistry, Chinese Academy of Science, Renmin Road 5625, 130022, Changchun, China. E-mail: xchen@ciac.ac.cn, ttang@ciac.ac.cn*
[b] *Institute of Chemical and Environment Engineering, West Pomeranian University of Technology, ul. Pulaskiego 10, 70-322, Szczecin, Poland*
[c] *Department of Physics and Materials Science, City University of Hong Kong, Tat Chee Avenue, Kowloon, Hong Kong, China*
[d] *Research Center of Nano Science and Technology, Shanghai University, Shanghai 200444, China. E-mail: dszhang@shu.edu.cn*

† Electronic supplementary information (ESI) available: Detailed experimental procedures including catalyst preparation, characterization (TEM), and the methods of catalytic activity tests. See DOI: 10.1039/c6cc08598a

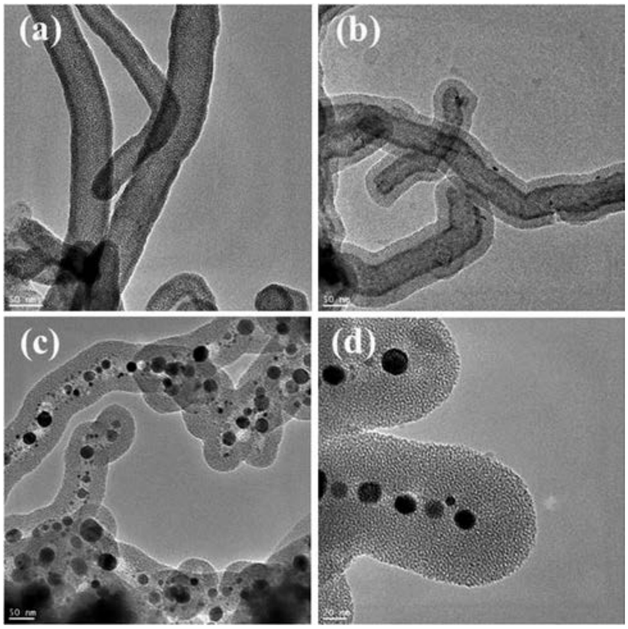

Fig. 2 TEM images: (a) CNT/Pd, (b) CNT/Pd@m-SiO_2, and (c and d) peapod structured Pd@m-C/SiO_2.

peapod structure, the Pd nanoparticles have a mean diameter of 15 nm and the outer mesoporous layer is composed of carbon and silica. The Pd nanoparticles have high stability during annealing due to confinement rendered by the outer mesoporous layer which stabilizes the Pd nanoparticles and protect them from aggregation.

The structure of the Pd@m-C/SiO_2 is determined by X-ray diffraction (XRD). As shown in Fig. 3a, the strong diffraction peaks at 40.1°, 46.7°, and 68.7° can be indexed to the (111), (110), and (100) reflections of crystalline Pd (0), respectively,[5] and metallic Pd is produced during annealing. The peak at 40.1° has the highest intensity and the (111) plane is the dominant crystal facet. The diffraction peaks at 26° and 22° correspond to the (002) planes of graphite and amorphous silica, respectively[21] and the intense diffraction peak at 2.75° (100) observed from the small-angle region indicates the formation of the ordered silica-mesostructure in the peapod structure.[22] The N_2 sorption/desorption evaluation shows that the peapod structure has a characteristic type IV isotherm. The total surface area on Pd@m-C/SiO_2 is as large as 537 $m^2\ g^{-1}$ confirming the mesoporous structure (Fig. 3b) consistent with XRD. The pore sizes are 1.6 and 3.7 nm according to the Barrett–Joyner–Halenda (BJH) method as shown in Fig. S2 (ESI†). The mesoporous structure allows the reactants to access the Pd nanoparticles and the products to exit through the mesopores. In addition, the metal interface may be exploited to boost the catalytic performance.[11]

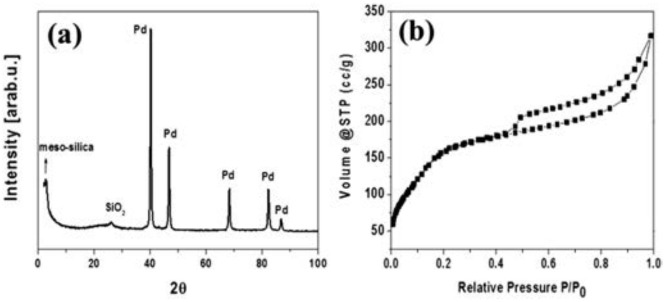

Fig. 3 (a) XRD pattern of the peapod structured Pd@m-C/SiO_2; (b) N_2 sorption/desorption profile of the peapod Pd@m-C/SiO_2.

To determine the catalytic activity and stability, the catalytic performance of Pd@m-C/SiO_2 is investigated by conducting catalytic reduction of nitrobenzene to aniline with H_2 in the model reaction.[23–25] The commercial Pd/AC (10 wt%) serves as the reference for comparison (Fig. 4). When Pd/AC is the catalyst in the reduction of nitrobenzene, conversion of nitrobenzene decreases from 100% to 82.6% after 10 cycles. However, the conversion rate of nitrobenzene is retained at 99.8% after 10 cycles for the Pd@m-C/SiO_2 catalyst providing evidence that the catalytic efficiency of Pd@m-C/SiO_2 is better than that of Pd/AC. To further demonstrate the advantage of the peapod Pd@m-C/SiO_2, the selectivity of the two catalysts is investigated by reduction of nitrobenzene to aniline as shown in Fig. 4b. After 10 cycles, the selectivity of the Pd/AC catalyst drops to 94.2% whereas that of the Pd@m-C/SiO_2 catalyst is stable at 99.8%. Hence, the peapod structure is better than the commercial Pd/AC catalyst in terms of the catalytic efficiency, selectivity, and stability. After each reaction, the Pd@m-C/SiO_2 catalyst can be easily separated from the reactants without leaching of Pd species but on the other hand, it is difficult to recover the Pd/AC catalyst from the organic solvent.

To further demonstrate the advantage of the peapod Pd@m-C/SiO_2 catalyst, NO is reduced by NH_3 in the presence of the Pd catalyst at 200 °C as shown in the following:

$$4NO + 4NH_3 + O_2 \rightarrow 4N_2 + 6H_2O.$$

Selective catalytic reduction of NO with NH_3 is an effective and economical method to eliminate NO_x and Pd has been demonstrated as the active component in catalytic reduction of NO.[26–28] In the presence of the Pd@m-C/SiO_2 catalyst, the conversion of NO is kept at 90% for 7 h continuously but that with the Pd/AC catalyst drops to 73% after 7 h illustrating the advantage of the former under the same conditions. The catalytic activity is mainly attributed to the degree of dispersion of the Pd nanoparticles. In addition, owing to the weak adhesion of Pd nanoparticles on the AC support, the Pd nanoparticles can migrate and agglomerate during the reactions leading to reduced catalytic

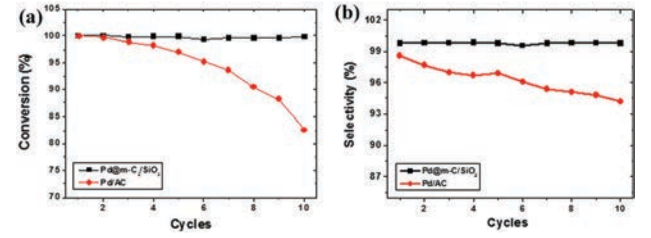

Fig. 4 Comparison of the two catalysts in the reduction of nitrobenzene with H_2 (Pd@m-C/SiO_2) (black line) and Pd/AC (red line): (a) conversion and (b) selectivity.

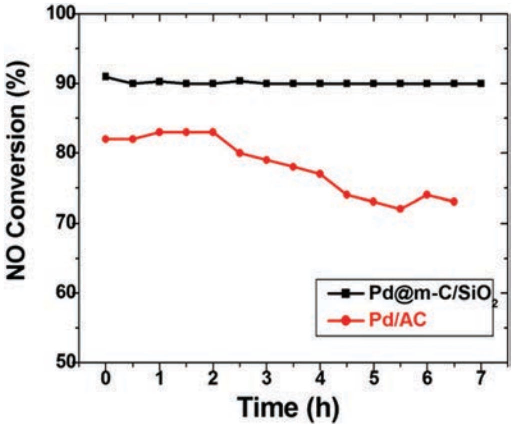

Fig. 5 Comparison of the two catalysts during reduction of NO with NH_3 in the presence of Pd@m-C/SiO_2 (black line) and Pd/AC (red line).

activity. After a mesoporous C/SiO_2 layer is formed, NO conversion in the presence of the Pd@m-C/SiO_2 catalyst is enhanced significantly and it can be explained by that the mesoporous C/SiO_2 sheath serves as a good support to improve dispersion of the Pd nanoparticles as well as an effective barrier to prevent aggregation of Pd nanoparticles (Fig. 5).[29,30]

The experimental results obtained from the two catalysts provide information on why the peapod Pd catalyst is better than the Pd/AC catalyst. In the peapod structure, the Pd nanoparticles are trapped in the m-C/silica nanotubes which prevent the Pd nanoparticles from aggregating into bigger nanocrystals and the m-C/silica wall is stable even at a high temperature. The porous wall not only leads to high activity of the Pd nanoparticles, but also accumulates more reactants to react with the Pd nanoparticles. This mitigates the formation of products on the Pd catalyst to deactivate the catalyst.

The peapod Pd@m-C/SiO_2 embedded with Pd nanoparticles shows high stability and selectivity and is a good high-temperature catalyst. The unique peapod structure with an outer mesoporous C/SiO_2 layer not only protects the Pd nanoparticles from aggregating, but also provides the mesoporous channels for molecules to access the Pd nanoparticles. The catalysts is stable at high temperature in long reactions. The Pd@m-C/SiO_2 catalyst also shows excellent catalytic selectivity and stable catalytic activity as observed from the reduction of nitrobenzene to aniline with H_2 as well as NO reduction by NH_3. The Pd@m-C/SiO_2 catalyst is very promising in high-temperature chemical reactions.

This work was financially supported by the Chinese National Science Foundation under project no. 51303170, National Science Centre of Poland under grant no. UMO-2015/18/E/ST8/00291, and City University of Hong Kong Applied Research grant (ARG) no. 9667122.

Notes and references

1 B. Lim, M. Jiang, P. H. Camargo, E. C. Cho, J. Tao and X. Lu, *Science*, 2009, **324**, 1302–1305.
2 R. W. J. Scott, A. K. Datye and R. M. Crooks, *J. Am. Chem. Soc.*, 2003, **125**, 3708–3709.
3 Y. Zhang, X. Cui, F. Shi and Y. Deng, *Chem. Rev.*, 2012, **112**, 2467–2505.
4 J. He, I. Ichinose, T. Kunitake, A. Nakao, Y. Shiraishi and N. Toshima, *J. Am. Chem. Soc.*, 2003, **125**, 11034–11040.
5 X. Chen, Y. Hou, H. Wang, Y. Cao and J. He, *J. Phys. Chem. C*, 2008, **112**, 8172–8176.
6 P. Granger and V. I. Parvulescu, *Chem. Rev.*, 2011, **111**, 3155–3207.
7 H. Ohde, C. M. Wai, H. Kim, J. Kim and M. Ohde, *J. Am. Chem. Soc.*, 2002, **124**, 4540–4541.
8 A. M. Tafesh and J. Weiguny, *Chem. Rev.*, 1996, **96**, 2035–2052.
9 C. S. Yeung and V. M. Dong, *Chem. Rev.*, 2011, **111**, 1215–1292.
10 B. Yoon and C. M. Wai, *J. Am. Chem. Soc.*, 2005, **127**, 17174–17175.
11 X. Chen, H. Wang, J. He, Y. Cao, Z. Cui and M. Liang, *J. Nanosci. Nanotechnol.*, 2010, **10**, 3138–3144.
12 M. Crespo-Quesada, A. Yarulin, M. Jin, Y. Xia and L. Kiwi-Minsker, *J. Am. Chem. Soc.*, 2011, **133**, 12787–12794.
13 X. Huang, S. Tang, X. Mu, Y. Dai, G. Chen and Z. Zhou, *Nat. Nanotechnol.*, 2011, **6**, 28–32.
14 X. Huang, S. Tang, J. Yang, Y. Tan and N. Zheng, *J. Am. Chem. Soc.*, 2011, **133**, 15946–15949.
15 W. Niu, L. Zhang and G. Xu, *ACS Nano*, 2010, **4**, 1987–1996.
16 Y. Xiong, H. Cai, B. J. Wiley, J. Wang, M. J. Kim and Y. Xia, *J. Am. Chem. Soc.*, 2007, **129**, 3665–3675.
17 Y. Xiong, J. Chen, B. Wiley, Y. Xia, S. Aloni and Y. Yin, *J. Am. Chem. Soc.*, 2005, **127**, 7332–7333.
18 Y. Xiong, J. Chen, B. Wiley, Y. Xia, Y. Yin and Z. Y. Li, *Nano Lett.*, 2005, **5**, 1237–1242.
19 Y. Xiong, J. M. McLellan, J. Chen, Y. Yin, Z. Li and Y. Xia, *J. Am. Chem. Soc.*, 2005, **127**, 17118–17127.
20 A. Kim, S. Lim, D. H. Peck, S. K. Kim, B. Lee and D. Jung, *Nanomaterials*, 2012, **2**, 206–216.
21 X. Chen, R. Klingeler, M. Kath, A. A. El Gendy, K. Cendrowski, R. J. Kalenczuk and E. Borowiak-Palen, *ACS Appl. Mater. Interfaces*, 2012, **4**, 2303–2309.
22 D. Y. Zhao, P. D. Yang, D. I. Margolese, B. F. Chmelkab and G. D. Stucky, *Chem. Commun.*, 1998, 2499–2500.
23 W. W. Lin, H. Y. Cheng, J. Ming, Y. C. Yu, Y. Q. Wu and F. Y. Zhao, *J. Catal.*, 2012, **291**, 149–154.
24 Y. J. Gao, D. Ma, C. L. Wang, J. Guan and X. H. Bao, *Chem. Commun.*, 2011, **47**, 2432–2434.
25 J. Ming, H. Y. Cheng, Y. C. Yu, Y. Q. Wu and F. Y. Zhao, *J. Mater. Chem.*, 2011, **21**, 6654–6659.
26 Y. W. Lee and E. Gulari, *Catal. Commun.*, 2004, **5**, 499–503.
27 A. P. Ferreira, S. Capela, P. Da Costa, C. Henriques, M. F. Ribeiro and F. Ramôa Ribeiro, *Catal. Today*, 2006, **119**, 156–165.
28 G. Qi and R. T. Yang, *Catal. Lett.*, 2015, **100**, 243–246.
29 S. X. Cai, H. Hu, H. R. Li, L. Y. Shi and D. S. Zhang, *Nanoscale*, 2016, **8**, 3588–3598.
30 L. Zhang, D. S. Zhang, J. P. Zhang, S. X. Cai, C. Fang, L. Huang, H. R. Li, R. H. Gao and L. Y. Shi, *Nanoscale*, 2013, **5**, 9821–9829.